Proceedings of the 17th World Congress
The International Federation of Automatic Control
Seoul, Korea, July 6-11, 2008

Fast Shake Mixing Control with Low Air Entrainment

Masahiro Maeda * **Ken'ichi Yano** *

* *Department of Human and Information Systems, Gifu University*
1-1 Yanagido, Gifu, 501-1193 Japan, (e-mail: yano-kn@cc.gifu-u.ac.jp)

Abstract: In this study, a fast shake mixing control system that allows control of the quantity of air entrainment, involving low mechanical stress and fluid bubbling by means of the suppression the sloshing of a fluid's surface, is developed. Mixing by means of horizontal shaking in a circular motion is addressed, with a CFD simulator being used for analysis of the liquid's behavior, and the quantity of air entrainment during mixing evaluated. To design a fast mixing control system, the hybrid shape approach was applied. In addition, a 3DOF robot manipulator was used to achieve an arbitrary mixing trajectory and velocity. As a result, air entrainment caused by the sloshing of the liquid's surface is elucidated. The effectiveness of the mixing control technique employing sloshing suppression is shown by simulations and experiments.

1. INTRODUCTION

Agitation or mixing is an important basic operation for accelerating chemical reactions, dispersion, emulsification, and cell cultures in the fields of chemistry and biology. The primary devices used for mixing are an agitator that rotates an impeller and a shaker that shakes a vessel without using an impeller. Agitation using a variety of impellers has been reported many cases so far(Szalai et al. (2004)). However, in cell cultures, agitation involving an impeller breaks down cells or causes contamination because it overly disturbs a fluid(Takeda et al. (1994)). Particularly, animal cells, unlike microorganisms, e.g., escherichia coli, are vulnerable to mechanical stress. Therefore, a static culture with adhesive cells is generally used. This culture method, however, is often problematic in that it disturbs propagation because of the disproportionate amount of nutrients and intercontact between the cells.

In contrast, a shaker can be used as a bioreactor because it avoids these problems due to its lack of an impeller(Honda et al. (1997), Büchs and Zoels (2001)). In addition, shake mixing has advantages in that the vessel is easy to clean and is intended for high-mix low-volume mixing operations. For this type of mixing, Kato et al. (1994) reported the minimum circulating frequency for complete mixing and the complete suspension of solid particles in a shaking vessel(Kato et al. (1995)). However, there are no studies analyzing the air entrainment and controlling it dynamically, although air and oxygen entrainment performance is a important indicator in the mixing operations of a bioreactor.

In fact, low oxygen entrainment causes a decline in cell culture performance, therefore, the circulating frequency of mixing is increased to assure the necessary oxygen entrainment in general. However, increasing the circulating frequency too much causes cellular death because of oxidation which is caused by the sloshing and bubbling of the liquid surface or by the mechanical stress induced by mixing. Therefore, shake mixing cannot be operated fast as present.

Therefore, this paper describes the development of a fast mixing control system that allows the control of the quantity of air entrainment while inducing low mechanical stress and suppressing fluid bubbling. In this study, mixing using horizontal shaking in a circular motion is described, and a computational fluid dynamics (CFD) simulator is used for analysis of the liquid's behavior, while the quantity of air entrainment during mixing is evaluated. To design a fast mixing control system, the hybrid shape approach(Yano et al. (2005)) is applied. In addition, a 3DOF robot manipulator is used to achieve an arbitrary mixing trajectory and velocity.

2. FORMULATION OF A MIXING SIMULATOR

2.1 Summary of CFD Simulator and Simulation Condition

In this study, the fluid analysis software, *FLOW-3D* from *FlowScience inc.*, is used. This simulator is a fluid calculation software that analyzes the three-dimensional transient flows of compressible/incompressible viscous fluid, and can treat free surfaces. The free surface calculation is performed based on the Volume of Fluid (VOF) method(Hirt et al. (1981)). The Fractional Area Volume Obstacle Representation (FAVOR) method(Hirt et al. (1985)) is used for the shape matching of complicated obstacle. The validity of this simulator has been demonstrated in many studies(Savage et al. (2001)).

Water is used as the target fluid. Table 1 shows the physicality of water. Figure 1 shows an overview of the mesh setting, and Table 2 shows the parameters of mesh setting.

2.2 Method for Evaluating Mixing Time

The scalar value 1 is allotted to the upper layer of the fluid($H = 0.05 \sim 0.10$[m]), and 0 is allotted to the lower

Table 1. Fluid parameters of water

Fluid parameters	Water
Density [kg/m^2]	1000
Viscosity [Pa·s]	0.0010
Temperature of the Fluid [K]	293.2
Surface Tension [N/m]	0.073
Specific Heat [J/(kg·K)]	4190
Thermal Conductivity [W/(m·K)]	1000

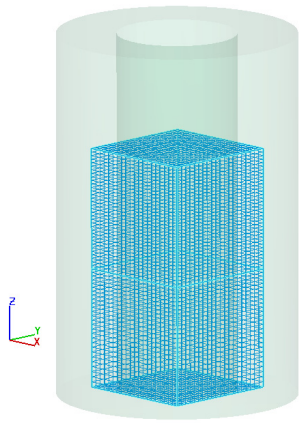

Fig. 1. Mesh setting of shaking vessel

Table 2. Mesh parameters

	X	Y	Z
Min. position[m]	0.000	0.000	0.000
Max. position[m]	0.100	0.100	0.200
Number of cell	20	20	60
Cell size[m]	0.005	0.005	0.003∼0.005
Total cells	24000		

layer($H = 0.00 \sim 0.05$[m]). As the mixing progresses, this scalar value converges to 0.5 by solving the advection equation. Figure 2 shows eight measurement points of the scalar value. The mixing time t_m is defined as the time when the scalar value has converged to 80 percent of 0.5 at every measurement point. In general, the more the criterion for convergence approaches 100 percent, the more the convergence is correct. However, as it approaches 100 percent, the calculation error of the simulation is dominant. Therefore, 80 percent is used as the criterion for convergence.

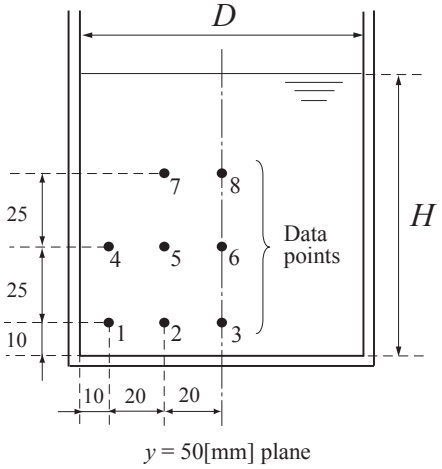

Fig. 2. Measurement points of shaking vessel

2.3 Evaluation of Air Entrainment

The quantity of air entrainment is a key indicator in the biochemistry field, but it is difficult to measure experimentally. In this paper, therefore, it is computed using a CFD simulator.

In this simulator, air entrainment at a liquid's surface is based on the concept that turbulent eddies raise small liquid elements above a free surface that may trap air and carry it back into the body of the liquid.

The air entrainment is expressed in (1).

$$A = \sum_{k=1}^{n} V_{ak} F_{fk} V_{fk} V_{ck} \tag{1}$$

where A is the quantity of air entrainment, V_a is the volume of air entrained per unit time, F_f is the fluid fraction, V_f is the volume fraction, V_c is the volume of the mesh cell, and n is the aggregate number of mesh cells.

3. MIXING CONTROL EXPERIMENT

3.1 Mixing Control System

The 3DOF manipulator that is used in the mixing operation is shown in Fig. 3. It has 3 links and joints, and thus has 3DOF. Each joint has a DC electrical motor working with an encoder. This manipulator can perform sensitive mixing that general shakers cannot. The cylindrical vessel is made of transparent acrylic and has an inner diameter $D = 0.1$[m]. The vessel is filled with liquid to a height $H = 0.1$[m].

Fig. 3. 3DOF manipulator for mixing

A circling trajectory is used for mixing, with a radius d of $0.005 \sim 0.020$[m], and a circling frequency N is $1.0 \sim 3.2$[s^{-1}].

The mixing time t_m was measured by the decolorization method using chemical reactions between iodine and sodium subsulfite. This method permits visualization of the mixing process as well.

3.2 Verification of the Mixing Simulator

Figure 4 shows the simulation results of the quantity of air entrainment in five seconds which was set at $N =$

$2.353[s^{-1}]$, and $d = 0.0146$[m]. Calculation time was about an hour by a personal computer (Pentiun D,3GHz). The mixing time was t_m=18.38[s], and the air entrainment was $A = 10 \times 10^{-7}$[-] at that time.

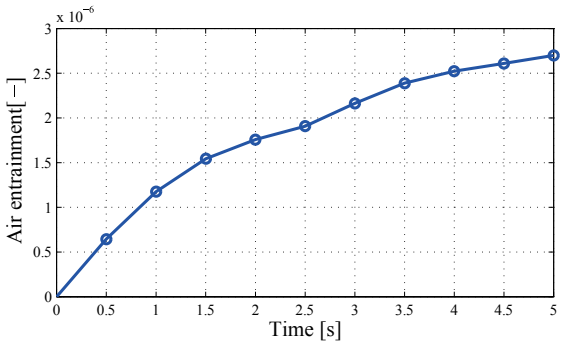

Fig. 4. Results of air entrainment; Case N=$2.353[s^{-1}]$ and d=0.0146[m]

As seen in the figure, the quantity of air entrainment at the start of mixing was larger than the amount seen later because angular velocity was constant. Figure 5 shows results of the shaking experiment and the simulation for a period of two seconds.

As the figure shows, the air bubbles are entrained because the liquid's surface is broken at the start of mixing. The quantity of air entrainment increases at a constant mixing state, but the trend is smaller than that seen at the start-up. A comparison of the mixing simulation with the experiment shown in Fig. 5 shows that the configuration of the free surface is reproduced with high accuracy by the CFD simulation. In addition, this simulator expresses air entrainment well because it shows the process at the same time point as in the experiment.

As a result, it can be said that this mixing control simulator can estimate not only the behavior of a liquid's surface but also can estimate air entrainment, thus avoiding the necessity of a controlled experiment. Hereafter, this simulator is used to design the control system aimed at achieving a fast mixing rate while reducing air entrainment.

4. MIXING CONTROL SYSTEM DESIGNED USING THE HYBRID SHAPE APPROACH

In order to design a controller that allows to follow the reference for angular velocity as fast as possible without sloshing, the hybrid shape approach is applied. In this approach, to solve an optimization problem using penalty terms expressed by the constraints of both the timedomain and the frequency domain, the time and frequency characteristics are fulfilled. In addition, this approach need not conduct feedback of the vibration data because the controller includes a notch filter at the natural frequency.

4.1 Identification of natural frequency by CFD simulation

The natural frequency of the vessel is used as notch frequency of the notch filter. This frequency is identified by analyzing the frequency characteristics of the sloshing of a liquid's surface calculated using *FLOW-3D*. In addition, the M-sequence signal, which is a pseudo-binary white noise signal, is used as the input voltage. This input provides single-axis acceleration, and causes liquid surface sloshing. The M-sequence signal is computed by (2), with a sampling time of 0.001[s], [a] simulation time of 2[s], a minimum input of 0[V], and a shift register number of 10.

$$(2^n - 1)\, T \leq T_{sim} \tag{2}$$

where T is the sampling time, T_{sim} is the simulation time and n is the shift register number. In addition, maximum input is set to 0.1[v] by a trial and error approach.

The sloshing behavior of the M-sequence signal and the result of the spectral analysis is shown in Fig. (6). In addition, sloshing is measured at $x = 0.09$, $y = 0.05$[m]. The natural frequency ω_n is identified $\omega_n = 2.93$[Hz] by the simulation results.

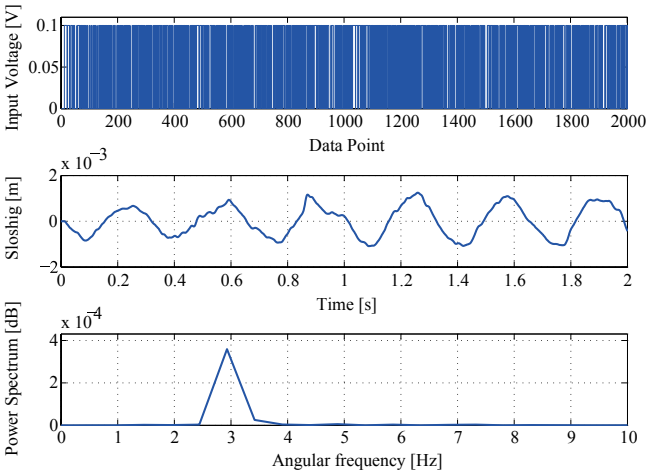

Fig. 6. Results of the spectrum analysis of the excitation simulations

4.2 Controller Design by Hybrid Shape Approach

The block diagram of the closed-loop system for the hybrid shape approach is shown in Fig. 7. This is a servo system that makes the angular velocity $\dot{\theta}$ of output follow the reference velocity $\dot{\theta}_{ref}$. The controlled system $G_m(s)$ denotes the transfer system, $G_v(s)$ denotes the vibration system, and $K(s)$ denotes the controller.

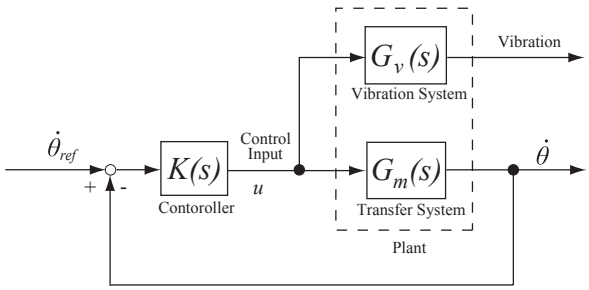

Fig. 7. Block diagram of velocity control

A proportional gain (K_I) and an integrator are selected as the first elements of the controller $K(s)$.

$$K_I(s) = K_I \frac{1}{s} \tag{3}$$

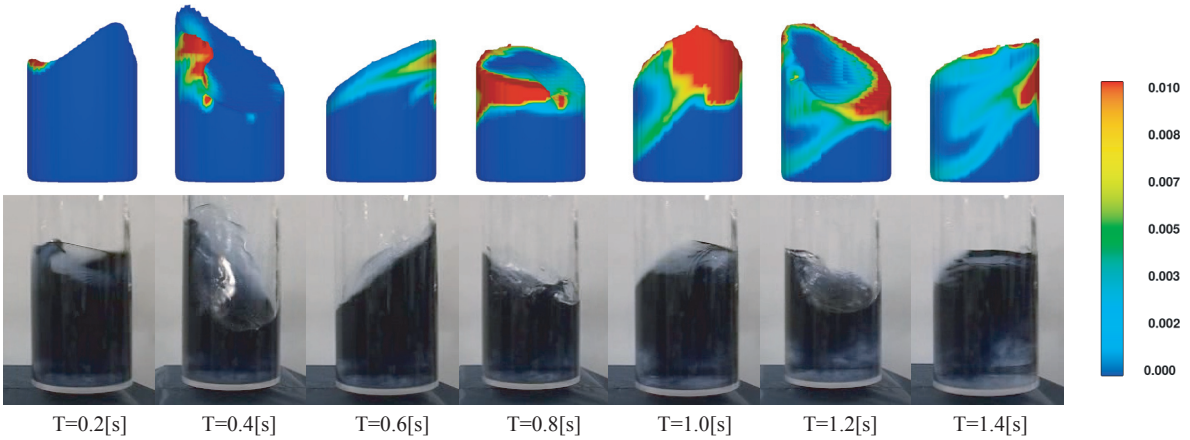

Fig. 5. Evaluation of shaking simulator

The notch filter is selected as the second element of the controller in order to suppress sloshing at the natural frequency. The parameter ζ is given as $\zeta = 0.0001$.

$$K_N(s) = \frac{s^2 + 2\zeta_N \omega_N s + \omega_N^2}{s^2 + \omega_N s + \omega_N^2} \tag{4}$$

In order to reduce the influence of higher-mode sloshing and noise, a low-pass filter (K_L), which makes the controller low gain in the high frequency domain, is selected as the third element of the controller.

$$K_L(s) = \frac{1}{T_L s + 1} \tag{5}$$

Finally, the transfer function of the controller which is multiplied by the above controllers is given as (6).

$$K(s) = \frac{K_I \left(s^2 + 2\zeta_N \omega_N s + \omega_N^2\right)}{s\left(T_L s + 1\right)\left(s^2 + \omega_N s + \omega_N^2\right)} \tag{6}$$

In (6), K_I and T_l are unknown parameters. These parameters are reasonably determined by solving an optimization problem.

In this approach, various control specifications in both the time and frequency domains can be given. The specifications of the controllers in both domains are formulated using penalty functions, and the controller $K(s)$ is then respectively calculated to satisfy the specifications. In this control design, Spec.(I) – Spec.(IV) shown below are given.

Spec.(I) The controller and closed-loop system are stable. Penalties are given in order to compensate for the stabilities of the controller and closed-loop system, if the following relations are unsatisfied, $Re[r_K] < 0$, $Re[r_{cl}] < 0$, $K_I > 0$, $T_l > 0$, where r_K and r_{cl} are the characteristic roots of the controller and those of the closed loop, respectively.

Spec.(II) The controller gain is less than 0[dB] at ω_l=314[rad/s], in order to decrease the influence of the higher-order sloshing mode and noise. Penalties are given if the following relation is unsatisfied, $|K(\omega_l)| < 0$[dB].

Spec.(III) The controller gain is less than 0[dB] at the natural frequency ω_n. Penalties are given if the following relation is unsatisfied, $|K(\omega_n)| < 0$[dB].

Spec.(IV) Maximum overshoot does not exceed a magnitude of 0.005[rad/s]. Penalties are given if the following relation is unsatisfied, $\max(O_s) < 0.005$[rad/s].

The controller's parameters are obtained by minimizing the cost function expressed in (7).

$$J = T_s + J_p \tag{7}$$

$$T_s = t \quad \text{subject to} \quad |\dot{\theta}_{ref} - \dot{\theta}| < \dot{\theta}_e \tag{8}$$

where T_s is the settling time, and J_p is the penalty term expressed in (9).

$$J_p = w_1 + w_2 + \cdots + w_i + \cdots \tag{9}$$

where w_i is the penalty. Each time the penalty conditions hold, the penalty w_i=10^8, which is large enough to avoid the penalty conditions, will be added to satisfy the control specifications.

4.3 Computation of a Controller

In order to obtain the controller, the optimization problem including the constraints is formulated with

- Target function : the settling time of the transfer T_s $\longrightarrow$ minimum
- Constraints : Spec.(I) – Spec.(IV).

Finally, the unknown parameters of the controller $K(s)$ are computed by solving the optimization problem with the constraints expressed in (7).

To optimize the cost function, the simplex method is applied to the present problem, because the number of unknown parameters are only two in this case, where the reflection coefficient α=1.0, the expansion coefficient β=0.5, the contraction coefficient γ=2.0, the circulating frequency $N = 2.4[\mathrm{s}^{-1}]$, and the reference angular velocity $\dot{\theta} = 2\pi N = 15.08$[rad/s]. The initial simplex values were $K_I = (10, 50, 2)$ and $T_L = (0.01, 0.005, 0.1)$. Figure 8 shows the results of the optimization of the cost function and the gain diagram of the controller. The results of the computations are $K_I = 13.08$, $T_L = 0.0181$, and the simulation results of the controller are shown in Fig. 9.

The reference trajectory shown in Fig. 10 was derived by integrating the angular velocity $\dot{\theta}$ and the radius gyration $d = 0.01$[m].

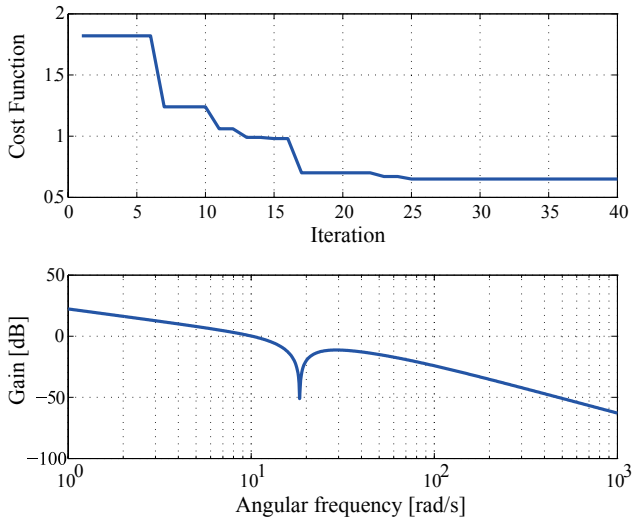

Fig. 8. Gain diagram of the controller and cost function

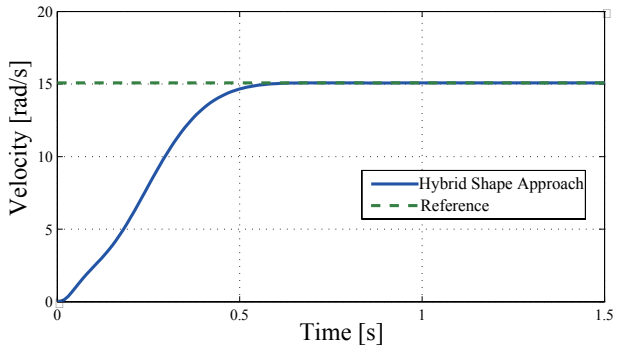

Fig. 9. Simulation result by the hybrid shape approach for $N = 15.08$[rad/s]

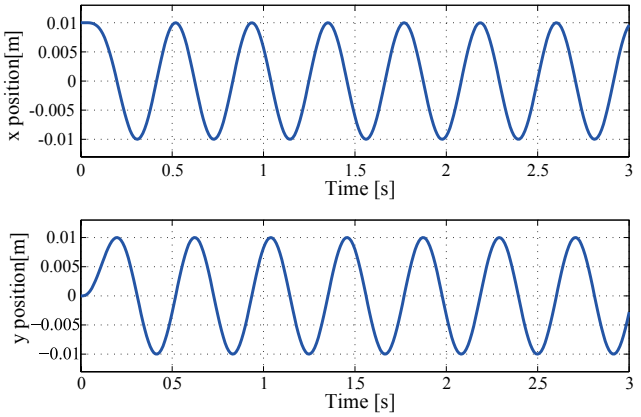

Fig. 10. Shaking path calculated by vibration damping angular velocity

5. MIXING CONTROL SIMULATION

The CFD was performed in order to estimate the sloshing suppression, mixing time t_m, and the quantity of air entrainment A during mixing using the hybrid shape approach. In addition, an uncontrolled mixing simulation was run to compare the sloshing suppression. The parameters used for the comparison were $N = 2.4[\mathrm{s}^{-1}]$, $d = 0.01$[m] in which the t_m was equal. As a result of the simulation, the t_m using sloshing suppression was $t_m = 23.65$[s], while that of uncontrolled mixing was $t_m = 24.15$[s].

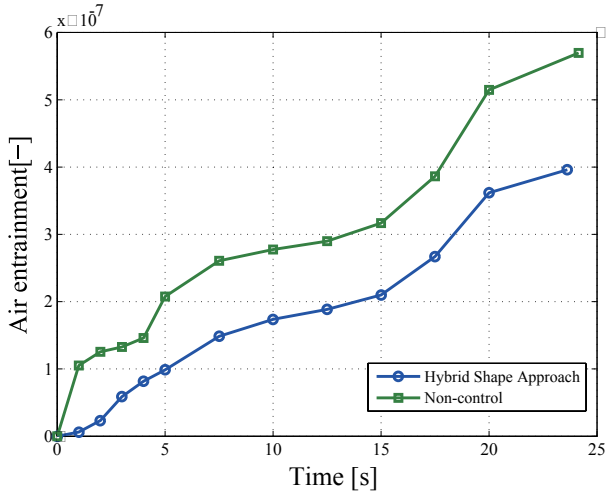

Fig. 11. The quantity of air entrainment

Figure 11 and Fig. 12 show the simulated results of air entrainment. As seen in the simulation results, the proposed mixing control method suppresses sloshing of the liquid's surface and reduces the quantity of entrained air.

6. CONTROL EXPERIMENT

Table 3 shows the mixing time t_m when using the decolorization method and the CFD simulation. As seen in the experimental results, t_m shows much the same pattern between the experiment and the simulation. Figure 13 shows a comparison between uncontrolled sloshing and the hybrid shape approach.

Table 3. Mixing time by using the decolorization method and the CFD simulation

	Simulation [s]	Experiment [s]
Hybrid Shape Approach	23.65	15
Non-Control	24.15	18

As the figure shows, the liquid surface is broke up greatly and entrains large air bubbles which can be visually confirmed in case of uncontrolled mixing. Meanwhile, mixing using the hybrid shape approach begins gently without the surface breaking up. From these results, it can be said that the sloshing of a liquid surface is bridled and the quantity of air entrainment is reduced by using the sloshing suppression control of the hybrid shape approach.

7. CONCLUSION

In this study, a fast mixing control system that enable to control a quantity of air entrainment is developed. And also, an evaluation method of a mixing time and an air entrainment of mixing are presented. For the fast mixing control system, a 3DOF robot manipulator is used and the Hybrid shape approach is applied. As a result, air entrainment caused by the liquid surface sloshing is elucidated. The effectiveness of the mixing control with sloshing suppression was shown by simulations and experiments.

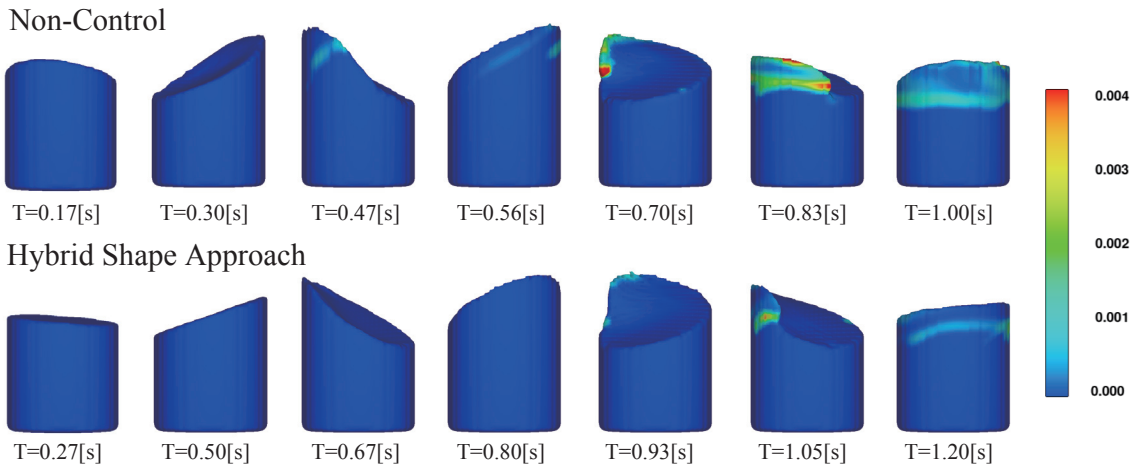

Fig. 12. Simulation result of air entrainment using the hybrid shape approach and non-control

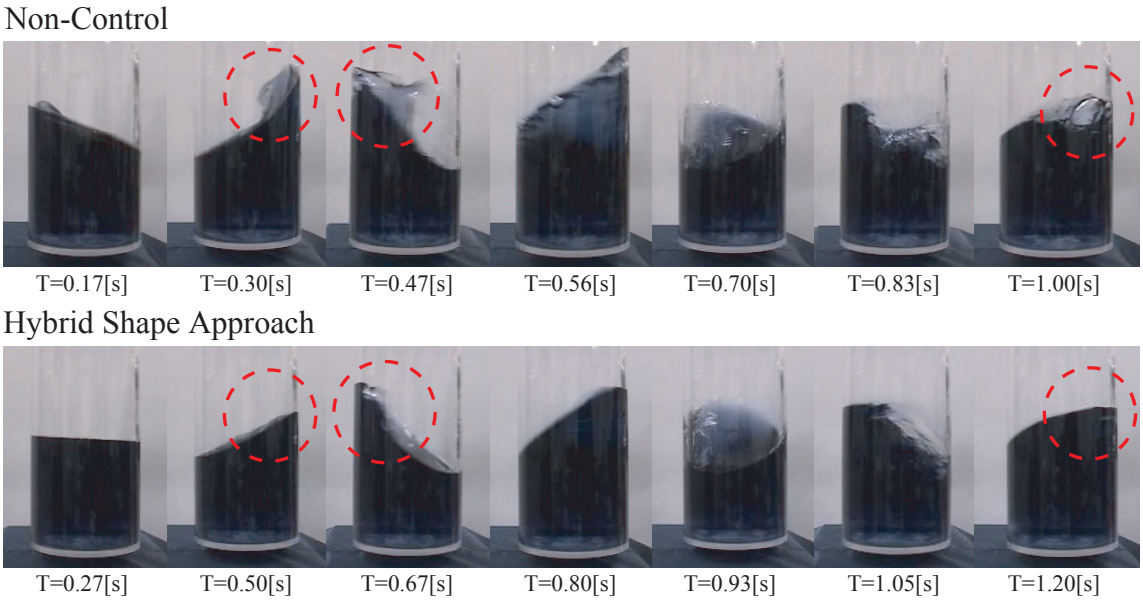

Fig. 13. Comparison between non-control and hybrid shape approach

REFERENCES

E. S. Szalai, P. Arratia, K. Johnson, and F. J. Muzzio. Mixing analysis in a tank stirred with Ekato Intermig impellers *Chemical Engineering Science* , volume 59, pages 3793–3805, 2004.

T. Takeda, M. Seki, and S. Furusaki. Hydrodynamic Damage of Cultured Cells of Carthamus Tinctorius in a Stirred Tank Reactor *J. Chem. Eng. Japan*, volume 27, pages 446–471, 1994.

H. Honda, T. Hattori, N. Uozumi, T. Kobayashi, Y. Kato, and S. Hiraoka. Production of Regenerated Plantlet using Shaking Vessel-Type Bioreactor *J. Chem. Eng. Japan*, volume 30, pages 179–182, 1997

J. Büchs and B. Zoels. Evalution of Maximam to Specific Power Consumption Ratio in Shaking Bioreactors *J. Chem. Eng. Japan*, volume 34, pages 647–653, 2001

Y. Kato, S. Hiraoka, Y. Tada, T. Mori, S. Shirai, T. Ue, and S. T. Koh. Mixing Time and Critical Circulating Frequency for Mixing of Low Viscosity Liquid in a Horizontally Shaking Vessel with Circulation Motion *Journal of the Society of Chemical Engineers Japan*(Japanese),volume 20, pages 437–444, 1994

Y. Kato, S. Hiraoka, Y. Tada, T. Shirota, S. T. Koh, Y. S. Lee, and T. Yamaguchi. Complete Suspension of Solid Particles in a Shaking Vessel for Solid-Liquid System *Journal of the Society of Chemical Engineers Japan*(Japanese),volume 21, pages 948–952, 1995

K. Yano, and K. Terashima. Sloshing Suppression Control of Liquid Transfer Systems Considering 3D Transfer Path *IEEE/ASME Trans. on Mechatronics*,volume 10, pages 8–16, 2005

C. W. Hirt, and B. D. Nichols. Volume of Fluid (VOF) Method for the Dynamics of Free Boundaries *Journal of Computational Physics*, volume 39, page 201, 1981

C. W. Hirt, and J. M. Sicilian. A Porosity Technique for the Definition of Obstacles in Rectangular Cell Meshues *Proc. of 4 th International Conference on Ship Hydrodynamics*, 1985

Savage, B. M, and Johnson, M.C. Flow over Ogee Spillway: Physical and Numerical Model Case Study *Journal of Hydraulic Engineering, ASCE*, August, pages 640–649, 2001